J Geophys (1988) 62:128–135

Journal of Geophysics

Investigation of non-linear tilt tides from the Charlevoix seismic zone in Quebec

J. Peters*[1] and H.-J. Kümpel[2]

[1] Oceanography Department, Dalhousie University Halifax, Nova Scotia, Canada, B3H 4J1
[2] Institute of Geophysics, Kiel University, D-2300 Kiel, Federal Republic of Germany

Abstract. Under certain conditions of crustal stress, non-linearities may be generated in the earth tide response. Non-linear constituents present in borehole tilt and tide gauge recordings from the Charlevoix seismic zone are studied in an attempt to discriminate between possible tectonically induced non-linear components and those resulting from non-linear interactions in the marine load tide. Mean tidal admittance estimates from harmonic analysis are compared with a loading model for constituents M_4 and M_6, and time-variant analysis is used to determine the temporal behaviour of the tilt and tide gauge admittances. Agreement between the model and mean admittance results, confirmed by some similarities in the tilt and tide gauge admittance time variations, indicates that crustal non-linearities are absent or undetectable. If laboratory observations of non-linear behaviour of highly stressed rocks are representative of in situ processes, then the apparent absence of non-linear tidal anomalies implies that the special situation in which the rate of change of the tectonic stress is equal to the mean tidal stress rate does not apply in the Charlevoix region. The experiments at Charlevoix have also allowed us to evaluate the spatial stability of non-linearities in the tidal tilt. Simultaneous recordings from two boreholes only 80 m apart show considerable discrepancies among many of the tidal constituents. It is speculated that local inhomogeneities in the granite country rock at the site are responsible for the anomalies.

Key words: Tidal tilt – Loading tides – Non-linear tides

Introduction

Most earth tide studies have been concerned with the linear response of the earth to the combined astronomical forcing and secondary tidal loading. In this study of borehole tiltmeter data from the Charlevoix seismic zone, we examine signal components in tidal data arising from non-linear processes either from a marine source (through loading) or resulting from possible non-linearity in the transfer function of the local crust. Our aim is to determine to what extent the observed non-linear components may be explained by: (a) crustal processes, (b) marine loading and (c) local inhomogeneities at the site.

The response of the earth to tidal forcing is generally described by infinitesimal linear elasticity theory. However, results from laboratory studies of brittle rock samples (Brace et al. 1966; Soga et al. 1978; Sobolev et al. 1978) have shown that at deviatoric stress greater than half the rock failure strength, volumetric strains arise due to the growth of microcracks (dilatancy). A number of models of non-linear elasticity have been proposed (Stuart, 1974; Mjachkin et al., 1975; Rice and Rudnicki, 1979) to explain both the laboratory results and field observations, in particular V_p/V_s precursors (Nersesov et al., 1969; Mjachkin et al., 1972; Whitcomb et al., 1973). As Beaumont (1978) points out, since the range of tidal stress (about 0.01 bar) is much smaller than the range of tectonic stress (about 5 kbar), the tidal response in this situation is essentially linear, though anisotropic, and governed by the state of the tectonic stress.

Scholz and Kranz (1974) showed in the laboratory that rocks subjected to cyclic loading at high deviatoric stress respond plastically and exhibit hysteresis; the energy loss is presumably due to the work against friction in opening and closing microcracks. Beaumont (1978) has described the possible effect on the tidal response where the tidal stress is superimposed on an accumulating tectonic stress field. In the case where the tectonic stress accumulation is either much less than or much greater than the mean tidal stress rate, the tidal response remains essentially linear. We should be able to distinguish between these two situations by examining the time dependence of the linear tidal response. If the response is constant then the tectonic stress, while possibly high, is only slowly varying or not varying at all. If the linear response is changing appreciably with time, this would imply that the tectonic stress rate is large and may be interpreted as being premonitory to rupture. Where the tectonic and mean tidal stress rates are approximately equal, the response is non-linear over the range of the tidal cycle. This would result in the generation of additional lines in the spectrum at sum and difference frequencies of the tidal constituents. These different styles of tidal response are therefore, in principle, diagnostic of the state of stress in the local crust. A study of time variations in the linear tidal response at Charlevoix (Peters and Beaumont, 1985) has not revealed an obvious tectonic signal, suggesting that the rate of tectonic stress accumulation is not large. It is among the aims of this study to determine

* *Present address:* Earth & Ocean Research Ltd., 22 Waddell Avenue, Dartmouth, Nova Scotia, Canada, B3B 1K3

Offprint requests to: H.-J. Kümpel

whether the tectonic stress rate is in the range of the tidal stress rate.

Agnew (1981) has studied the effect on the tidal response of intrinsic non-linearity in rocks based on evidence from seismic studies. He shows that for non-dissipative materials the strongest effect would occur at the second harmonic of the tidal constituents (for example M_4, the second harmonic of M_2), whereas for dissipative materials the effects would be generated at the odd harmonics (for example M_6, the third harmonic of M_2). The predicted non-linear strains (or tilts), however, are too small to be detected at the significance level of this study. It should be emphasized that this is a different problem from that described by Beaumont (1978). Whereas Agnew considers the intrinsic non-linearity of the rock, Beaumont is looking at non-linearity generated in response to applied stress close to the failure strength of the rock.

We must additionally consider the non-linear content of the tidal input. There have been numerous studies of non-linear harmonics in the marine tide (see, for example, Zetler and Cummings, 1967; Rossiter and Lennon, 1968; Gallagher and Munk, 1971). The prominent sources of these components are velocity and friction-dependent interactions in shallow water. Godin (1973) has made a detailed analysis of 8 years of tide gauge data from Québec City (150 km upstream from Charlevoix) showing the importance of the non-linear harmonics in the estuary. Since the observed tidal signal at Charlevoix is dominated by loading from the St. Lawrence estuary, there is abundant energy at the higher-order tidal harmonics (Peters and Beaumont, 1985), at least part of which must arise from shallow-water interactions. Another source of harmonics in the loading arises from rectification of the linear tide over drying areas (Zschau, 1979). This is not generally reflected in the tide gauge data since they are recorded in deep water.

Cavities, topography or geological inhomogeneities may produce strain-induced tilt anomalies that vary over short distances (Harrison, 1976). For example, Flach et al. (1975) reported an 8° phase difference in M_2 between two Askania borehole pendulums recording simultaneously in 15-m and 30-m boreholes located 10 m apart. Characteristics of the temporal variation of non-linear tides due to tectonic stress build-up or marine loading should not be masked by these local effects. They will merely result in constant phase shifts and/or constant amplitude differences between installations at various locations.

In this study we compare the mean amplitudes and Greenwich phase lags of M_4 and M_6 determined from the borehole tilt recordings taken at Charlevoix Observatory, with theoretical estimates based on a loading model of the St. Lawrence estuary. Time-variant analysis results of the tilt and nearby tide gauge data are compared to see to what extent the stability of the tidal tilt response is determined by the loading input. Finally, we consider local effects that distort the crustal tilt response in the vicinity of the site.

Data and analysis

The tilt data were recorded in two boreholes 80 m apart and 47 m deep, using Bodenseewerk (formerly Askania) borehole pendulums (Peters and Beaumont, 1985). The study was done in two parts: one using tide gauge data available from May 1, 1981 to December 31, 1982 and tiltmeter data from November 27, 1981 to July 24, 1983 for determining the spectral characteristics of the non-linear constituents; and the second using tilt and tide gauge data for all of 1983 for the mean admittance and time-variant analysis. The 1983 data set was used for the time-variant analysis because of the small number of gaps during that period, a factor which has considerable influence on the accuracy of the results. Table 1 lists details of the data analysed; Fig. 1 shows the relevant locations.

Table 1. Data used in this study

Tilt	
Borehole 1	Nov. 27, 1981–Dec. 31, 1983
Borehole 2	Nov. 27, 1981–Dec. 31, 1983
Tide Gauge	
St. Joseph de la Rive	May 1, 1981–Dec. 31, 1983
Tadoussac	Jan. 1, 1983–Dec. 31, 1983

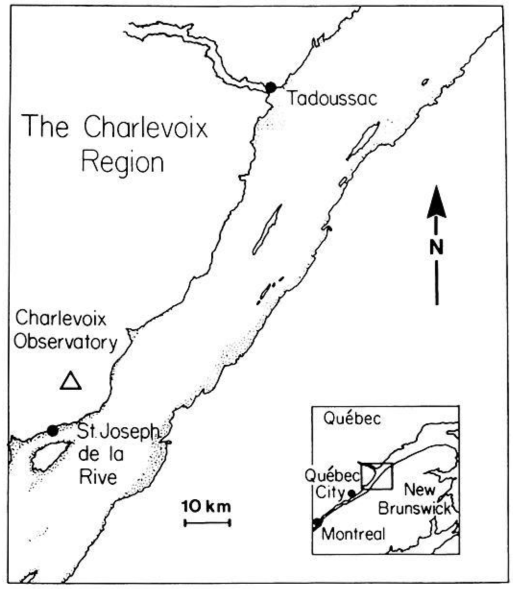

Fig. 1. Map of the St. Lawrence estuary near the Charlevoix observatory. The *stippled areas* are beaches. The location of the observatory is 47° 32.9′N, 70° 19.3′W

An adaptation of the Goertzel algorithm (Goertzel, 1958) was used to compute the amplitude spectra. Unlike the fast Fourier transform, the Goertzel method permits the rapid calculation of the direct Fourier transform for arbitrary frequencies for a time series of any length, without the need to process frequencies over the entire spectrum. The computation was done on a bandpass-filtered time series which had been multiplied by the Hanning window, so that the spectral resolution is $dw = 4\pi/(NdT)$, where dT ($=1$ h) is the sampling interval of the data and N the number of hourly data points. Distortions from data gaps were reduced by filling the gaps with harmonic constituents from a preliminary Fourier transform that was applied to data series with linearly interpolated gaps.

For the time-variant analysis, we have used the HYCON tidal harmonic analysis program of Schüller (1977). The data from 1983 were divided into overlapping 60-day subsets with the origin shifted for each set by 10 days. The output of the program is a sequence, for each tidal harmonic, of amplitude and phase estimates derived from ana-

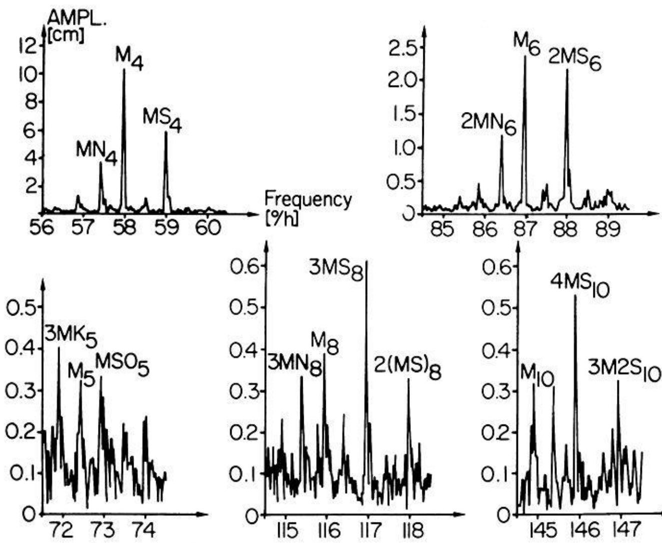

Fig. 2. High-resolution amplitude spectrum (0.05°/h bandwidth resolution) of St. Joseph de la Rive, showing the main non-linear tidal bands

lysis of the subsets, which together form a time-varying admittance function. A detailed description of the method is given in Peters and Beaumont (1985).

The marine tide

Spectrum of the marine tide

Figure 2 shows the amplitude spectrum for tidal frequencies greater than 56°/h (43 μHz) of the tide gauge at St. Joseph de la Rive for the period May 1, 1981 to December 31, 1982. Because of its close proximity to the site (Fig. 1), this tide gauge is representative of a major part of the loading at Charlevoix. The background noise level decreases from 0.3 cm within the quarter-diurnal band to 0.15 cm in the tenth-diurnal band.

Other tide gauge recordings in the estuary are shorter (in some cases less than 600 h), resulting in a lower spectral resolution. Adjacent frequencies then modulate one another, which for the shorter sets leads to biased estimates for the amplitudes and phases. Only M_4 and M_6 are free of significant interference within a bandwidth of 0.5° /h (0.386 μHz). It is for this reason that these frequencies were chosen for the comparison between the loading model and the observed mean amplitudes and phases; and for the time-variant analysis of 60-day (0.5°/h resolution) subsets of the 1983 data.

Tidal loading model

The load tilt calculations were made by the same method as Peters and Beaumont (1985) using the same triangular subdivision of the St. Lawrence estuary, but excluding the Saguenay River west of Tadoussac. The Green functions for the point load response of the Farrell Gutenberg Bullen Earth model (Farrell, 1972) were used and the integrated effect of the marine tide distribution found by convolving the Green functions with the in-phase and quadrature components of the discretized marine tide distribution. Calculations were made for the two extreme cases in which drying areas remain either wholly dry or wholly submerged. Realistic loading predictions will be affected by partial drying and should lie somewhere in between the extremes.

For the reasons mentioned above, empirical cotidal charts, based on observations from coastal tide gauges, were drawn for the non-linear constituents M_4 and M_6 only (Fig. 3a and b). Since the quarter- and sixth-diurnal tides are generally a localized shallow-water phenomenon, ocean areas beyond the mouth of the estuary were not included in the tidal distribution. Within the estuary, however, we have taken the liberty, in the absence of sufficient coastal gauges and the total lack of mid-stream stations, to freely interpolate co-amplitude and co-phase lines across the river. There is some justification for this. The across-stream depth profile is shallow on the south-eastern two-thirds (ranging from 0 to 5 m) throughout the middle part

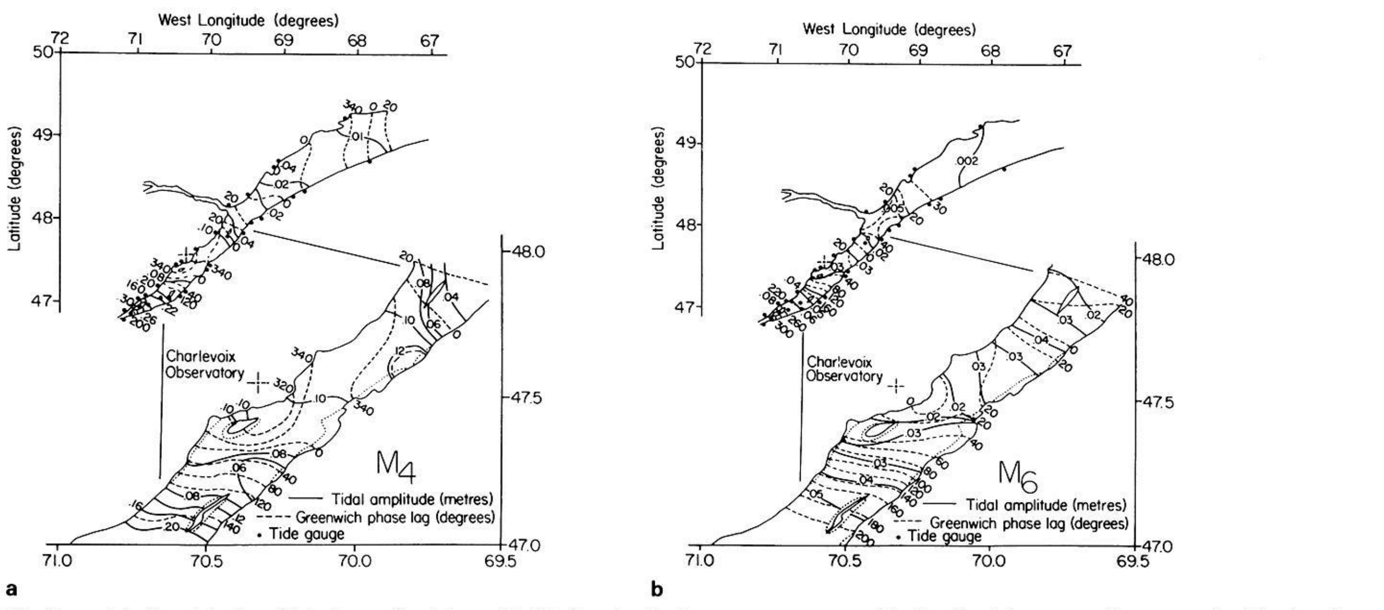

a **b**

Fig. 3a and b. Empirical cotidal chart of **a** M_4 and **b** M_6 for the St. Lawrence estuary, with detail of the area adjacent to the Charlevoix site. *Dots* mark the location of tide gauge installations

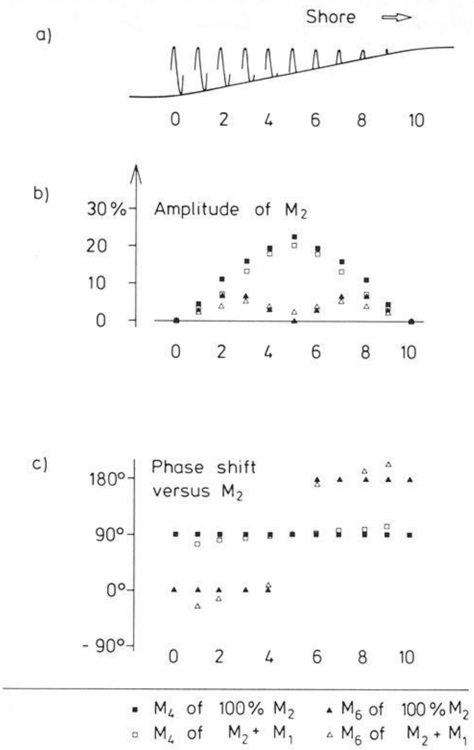

Fig. 4. a Schematic of a ramp-like beach showing the truncation of the linear tide as a function of position. **b** Relative amplitude of second- and third-order harmonics M_4 and M_6 of the simulated semi-diurnal M_2 tide plotted against position. **c** Phase shift of second- and third-order harmonics M_4 and M_6 of the simulated semi-diurnal M_2 tide plotted against position. Calculations were made for truncation of a single semi-diurnal wave of amplitude 1.0 (*full symbols*) and truncation of a combined 0.3-amplitude diurnal and 1.0-amplitude semi-diurnal wave series (*open symbols*), more closely resembling the real situation at Charlevoix

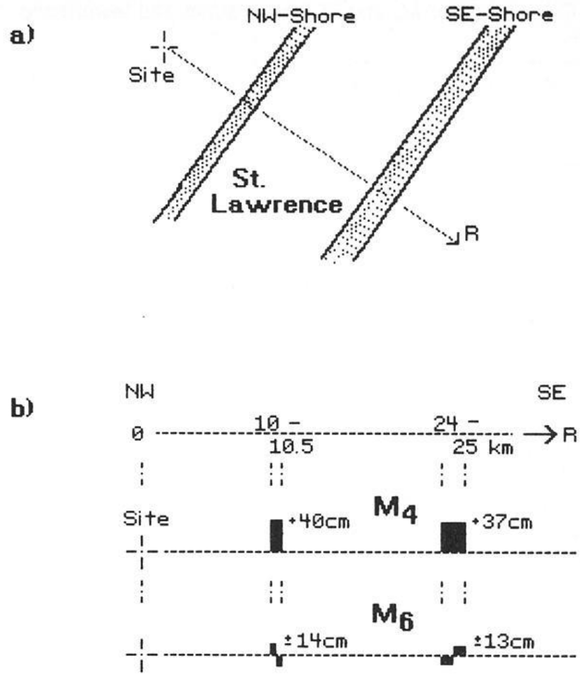

Fig. 5 a and b. Geometry for loading calculations of rectified linear tide. **a** Strip-like beaches at 10.0–10.5 km and 24–25 km distance *R* from the site at the banks of the St. Lawrence River. **b** Maximum loading amplitudes over the whole beaches for the second-order harmonic M_4 and phase reversal midway up the beach for the third-order harmonic M_6

of the estuary, the deeper water being restricted to a channel along the north shore. We expect, therefore, non-linear interactions to occur throughout much of the shallow expanse. The least reliable part of the cotidal maps is in the area to the south of the Charlevoix site in which the steep gradient in amplitude and phase lag, for both constituents, is based on data from only two reliable tide gauges. This area clearly has the largest influence on the south tilt component, so that these results should be interpreted with caution.

Rectification of the linear tide

The non-linear tide loading model takes no account of rectification of the linear marine tide over drying areas. To estimate the effect on the loading, we simulated the truncation of the linear tide on a ramp-like beach (Fig. 4a). A set of 11 time series were synthesized to represent the tide at positions up the profile of the beach. Each series consisted of either a single sinusoid at semi-diurnal or two sinusoids at diurnal and semi-diurnal frequencies. Each series was then truncated using a gate function, the gate width determined according to position on the beach. The resulting series were Fourier transformed and amplitudes and phases of the second and third harmonics of the semi-diurnal tide (simulating M_4 and M_6) were plotted as a function of position on the beach (Fig. 4b and c). While the relative amplitudes of the harmonics, the second in particular, are quite high, there is a phase reversal of the third harmonics midway up the ramp, which results in a degree of cancellation. We will now use these results to arrive at a worst-case estimate of the effect of linear tide rectification on the non-linear loading at Charlevoix.

In the vicinity of the Charlevoix site, the width of the beaches, or drying areas, is small compared with their distance from the site. We calculated the loading tilt resulting from a 0.5-km-wide beach on the NW bank and a 1-km-wide beach on the SE bank of the St. Lawrence River (Fig. 5a). The amplitude of the marine M_2 amounts up to 2 m on the NW shore and up to 1.85 m on the SE shore (Peters and Beaumont, 1985). Taking 20% of this amplitude over the whole beach as a worst case for the second harmonic from Fig. 4b or 7% for the third harmonic, respectively, and considering partial cancellation due to phase reversal for the latter (Fig. 5b), we arrive at maximum effects of 30% of the loading model estimate of M_4 and 0.2% of the loading model estimate of M_6 (see next section). If, however, the whole drying areas were at heights represented by position 2 or 8 in Fig. 4a, no cancellation for the third-order harmonic would occur. The maximum effect could then be 40% of the loading model estimate of M_6. Therefore, a significant input from the rectification of linear tides over tidal flats cannot be excluded.

The tilt tide

Comparison of mean tidal estimates

The mean tidal estimates from the HYCON analysis of the 1983 data from boreholes 1 and 2 are compared with

Table 2. Comparison of M_4 and M_6 observations and loading model results

	Borehole 1		Borehole 2		Loading model			
					100%		0%	
South								
M_4	2.19 ±0.08	(340.2) ±3.9	3.08 ±0.11	(339.5) ±3.1	3.16	(341)	3.76	(340)
M_6	0.40 ±0.05	(98) ±7	0.44 ±0.06	(77) ±7	0.79	(68)	0.93	(64)
East								
M_4	6.80 ±0.17	(352.7) ±1.9	7.77 ±0.20	(352.9) ±2.1	6.53	(345)	6.84	(346)
M_6	1.58 ±0.08	(25.4) ±3.8	1.87 ±0.14	(22.8) ±5.0	1.68	(23)	1.78	(24)

Amplitude in nanoradians, Greenwich phase lag (brackets), 95% confidence limits

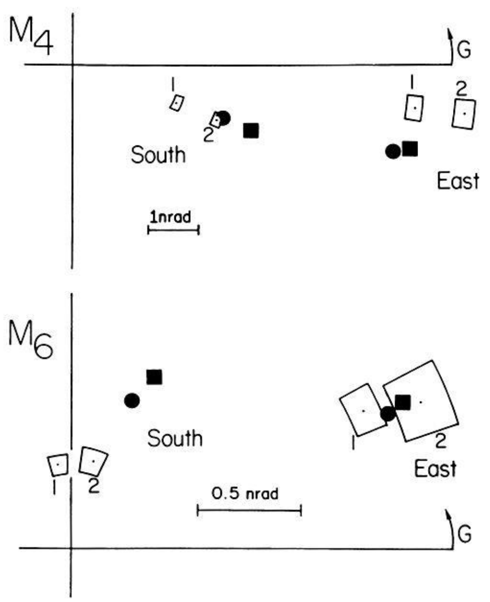

Fig. 6. Phasor plots of the M_4 and M_6 mean admittance estimates derived from the HYCON analysis of the south and east components of tilt measured in boreholes 1 and 2. The *solid dots* represent the loading model predictions for the two extreme cases in which there are no drying areas (*square dots*) and areas that do dry, doing so completely (*round dots*). Error sectors around each of the estimates are based on 95% confidence limits. *G* is Greenwich phase lag

the loading model predictions shown in Table 2. The results are displayed in the form of phasor diagrams in Fig. 6. Body tide amplitudes for M_4 are only 0.0059 nrad in EW and 0.0045 nrad in NS, using the development of Xi (1987), and even smaller for M_6. They are far beyond the resolution of the tilt measurements.

Apart from M_6 from the south direction, the borehole 1 results are systematically smaller in amplitude than those of borehole 2, but are consistent in phase. The loading model results are in reasonable agreement with the observations, except in the case of M_6 south. For M_4 east the model favours borehole 1, although both observations lag the theory by about 7°. For the south direction the model

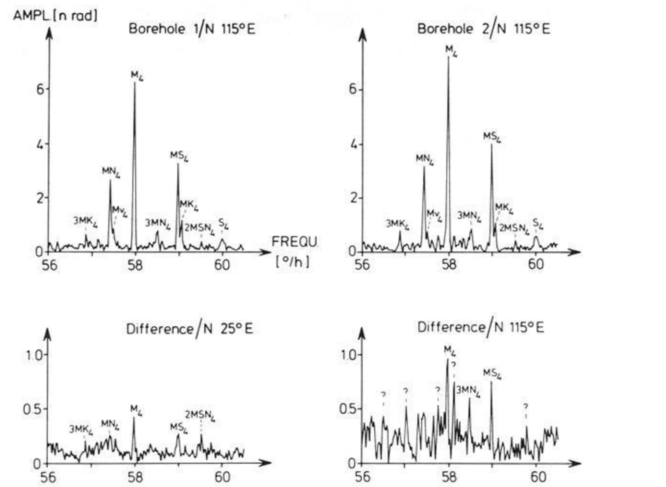

Fig. 7. High-resolution quarter-diurnal amplitude spectra (0.05°/h bandwidth resolution) of tilt in boreholes 1 and 2 and of the difference tilt signal at azimuth grossly parallel (N25°E) and perpendicular (N115°E) to the St. Lawrence River. N115°E is the azimuth at which most of the quarter-diurnal signal energy is observed

appears to overestimate the loading by as much as 100% for M_6 and by 70% and 20% for M_4 in boreholes 1 and 2, respectively, although we cannot rule out the possibility that local effects may be partly or wholly responsible for the disagreement.

Below, we examine more closely the coherency between the two borehole measurements to establish whether the differences are due to instrumental effects such as calibration or uncertainties in orientation.

Local tilt anomalies

Quarter-diurnal spectra of 20 months tilt recordings in boreholes 1 and 2 are plotted in Fig. 7. They essentially show the same tidal peaks as the tide gauge recordings in the St. Lawrence River (Fig. 2). A significant difference, however, can be seen between the tilt signals from the two boreholes. Spectra of the difference tilt signal contain non-linear tidal energy that seems to be polarized close to the azimuth of strongest marine loading.

Using the south and east admittances determined from both boreholes, we can derive the observed and difference tilt ellipses for each constituent (Tomaschek and Groten, 1963). The difference tilt for each constituent is formed from the difference between the admittance observed in boreholes 1 and 2. The ellipses are shown for the linear tides O_1, K_1, S_2, M_2 and N_2 in Fig. 8a and for the non-linear constituents MS_4, M_4, MN_4, $2MN_6$ and M_6 in Fig. 8b.

The observed ellipses for all constituents are strongly polarized towards the loading and in all cases, except the diurnals, the major axis for borehole 2 is larger. The most striking feature of these data is the polarization of the difference tilt ellipses (or tilt anomalies). The major axes of the linear tide anomalies lie in the range 60°–80° azimuth, whereas those of the non-linear anomalies are confined to azimuths in the range 110°–140° (see Fig. 9). Obviously, the linear tide anomalies (composed of body and loading components) are polarized 45°–60° anticlockwise with respect to the azimuth of the forcing, and the non-linear tidal anomalies are polarized 15°–40° clockwise with respect to the load only forcing. Calibration errors would result in

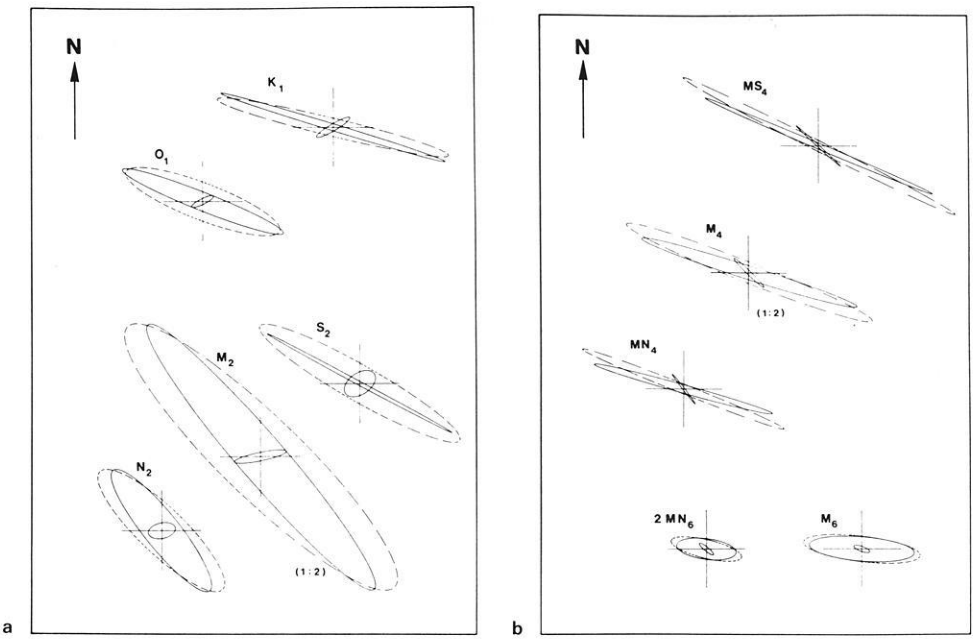

Fig. 8 a and b. Tilt ellipses of the observed tilt in borehole 1 (*full line*) and borehole 2 (*dashed line*) and the difference tilt shown for **a** linear tidal constituents, and **b** non-linear constituents. M_2 and M_4 are plotted on a double scale relative to the other constituents. The lengths of the lines in the centres of the ellipses are 24 nrad (48 nrad for M_2) in **a** and 2.4 nrad (4.8 nrad for M_4) in **b**

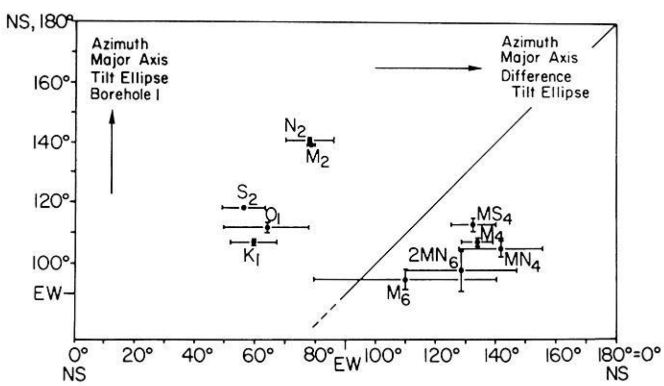

Fig. 9. Orientation of observed tilt ellipses for constituents measured in borehole 1 versus the orientation of the tilt ellipses for the same constituents of the difference between boreholes 1 and 2. Error bars reflect 95% confidence limits

anomalies aligned with the observed tilt ellipses (such anomalies would appear close to the oblique line running through the upper right corner in Fig. 9). Alignment errors of one or both tiltmeters would introduce anomalies characteristic of each tidal species, dependent on their frequency as well as their spatial distribution. Instead, we find a distinct grouping into linear and non-linear tidal components.

The alternative explanation for the observed anomalies involves the presence of a subsurface structural inhomogeneity (fault, fracture, geological contrast etc.) near one of the boreholes, through which strain-tilt coupling generates an anomaly governed by the nature and distribution of the forcing function. That the non-linear anomalies are polarized close to the azimuth of the loading is consistent with strain-tilt coupling arising from the non-linear load strain. In contrast, the linear tide, which has a body tide component, will produce an anomaly which is a function of both the body and the load strain. Furthermore, since the forcing distribution (load and body tide) for the diurnal and semi-diurnal constituents are different, strain-tilt coupling effects should also be different. Evidence for this is seen in Fig. 9 in which N_2 and M_2 form a subgroup separate from O_1 and K_1. That S_2 does not appear to fit into the scheme may reflect the influence of additional perturbing inputs, such as atmospheric tides, which are dominant within this frequency band.

The existence of subsurface inhomogeneities is known from a third borehole 80 m from the other two, in which a major water-bearing fracture was encountered at a depth of 130 m. Also, a subsurface discontinuity is inferred in the vicinity of boreholes 1 and 2 from a 90° shift in electric field polarization angle determined from magnetotelluric measurements at the site (R. Kurtz, personal communication).

Time variations in the M_4 and M_6 admittances

Because of the need for data continuity in time-variant analysis (Peters and Beaumont 1985), we have analysed tilt and tide gauge data recorded during 1983 in which relatively small data loss occurs (in the St. Joseph de la Rive data at a level of 13% and in borehole 1 at 2.7%). Figures 10 and 11 show the time-varying admittances in the form of trajectories in phasor space for M_4 and M_6, estimated from the HYCON analysis of the south and east components of tilt and the tide gauges at St. Joseph de la Rive and Tadoussac.

For the east direction M_4 traces out an almost circular path, perhaps indicative of an annual component, with a range of 12% in amplitude and 11° in phase. While the south component admittance shows larger fractional changes (30%) than the east, the absolute range of the changes is approximately the same. Variations in each component are coherent between boreholes, suggesting that the tiltmeters are responding to a regional process. Also, from analysis 10 on, the south and east series behave in a similar way and, in terms of the phase lag with respect to the mean, are coherent with the variations at Tadoussac. There is no obvious correlation between the tide gauge at St. Joseph de la Rive and the other M_4 admittance trajectories.

The variations in M_6 are also coherent between bore-

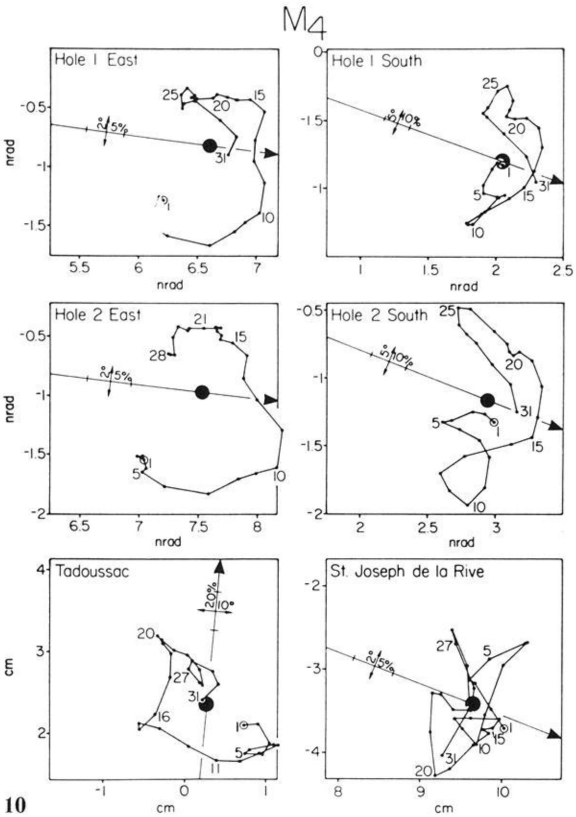

10

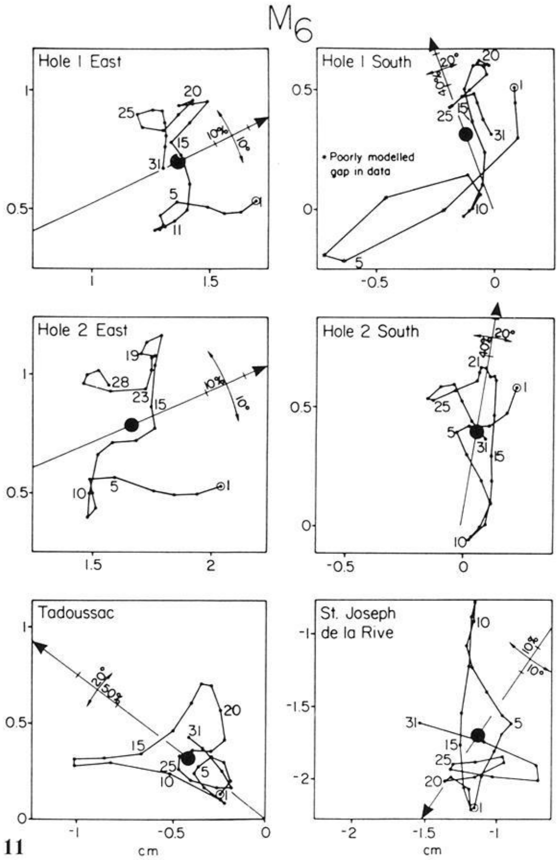

11

Fig. 10. Phasor trajectory plots of the M_4 admittance for tilt measured in boreholes 1 and 2 and tide gauges Tadoussac and St. Joseph de la Rive, estimated from HYCON sequential analysis. The mean admittance is indicated by the *round dot*. The *arrow* points in the direction of increasing amplitude. Fractional changes can be estimated from the amplitude and phase scales on the arrow which pertain to changes relative to the mean

Fig. 11. Phasor trajectory plots of M_6. Details as for Fig. 10

holes for each component direction. For the east direction the amplitude changes are mainly confined to the start and the end of the year, with the phase lag varying during the middle period. For the south direction, apart from an anomalous excursion in the borehole 1 curve caused by a gap, the variations are predominantly in amplitude and cover a range of 200% because of the small signal. Nevertheless, the essential features of the larger-amplitude east component remain, with the absolute changes being approximately the same in both directions. There is no clear correlation between the tide gauge at Tadoussac and the tilt. However, the sustained amplitude cycle dominating the tilt variations during the first 8 months (analyses 1–20) is also clear in St. Joseph de la Rive results.

Discussion and conclusions

Without embarking on a rigorous and probably futile investigation of the inhomogeneous local strain field geometry at the Charlevoix site, we have established that the differences in the mean values of the non-linear tidal results for the redundant tilt observations are probably due to strain-tilt coupling and are not associated with instrumental effects.

Unlike most tidal studies which are concerned with explaining small perturbations in the tilt response, we are trying to find the source of the entire signal. The only non-tectonic source of the non-linear M_4 and M_6 tidal signal is from tidal loading. Agreement between the observed mean admittance and the loading model results suggests that detectable tectonically induced non-linearities are not being generated in the Charlevoix area. The only major discrepancy occurs in the south component for M_6 in which the observed is about 50% smaller than predicted. It is likely that errors in the model due to the poorly constrained tide distribution south of the site are responsible for the disagreement.

In general, the level of agreement between the time-varying tide gauge admittances and the corresponding tilt results is only fair. This may be due to the small spatial scale of the shallow-water interactions, which makes a comparison between individual tide gauges and the tilt generally inappropriate. Also, in the case of St. Joseph de la Rive, the analysis results for data sets 21–27 were derived from data with gaps and were consequently heavily biased by the interpolation model. However, taken together, the mean admittance results and time-variant analysis results strongly indicate a marine origin for the non-linear harmonics in the tilt.

If the arguments of Beaumont (1978) are realistic, this result implies that the special condition in which the rate of change of the tectonic stress is equal to the mean tidal stress rate does not apply during the period covered by this study, or is not detectable within the prominent background of the non-linear loading. In their study of linear tidal admittance variations, Peters and Beaumont (1985) found no evidence for a high rate of stress accumulation in the region. Thus, from the combined evidence of both tidal response studies, the regional tectonic stress is stable or only slowly changing. These results are not unexpected considering the low level of earthquake activity during the period of the tiltmeter experiment. During 1983, the largest earthquake in the region was of magnitude 3.8, the epicentre of which was 38 km from the observatory.

Acknowledgements. This project was supported by the Air Force Geophysics Laboratory, Hanscom AFB under contracts F19628-80-C-0032 and F19628-83-K-0023, the Natural Sciences and Engineering Research Council through Operating and Equipment grants to C. Beaumont, and the Division of Geophysics, Geological Survey of Canada. The Marine Environment Data Service provided the tide gauge data. We would like to thank Chris Beaumont and Walter Zürn for helpful discussions and criticism, Tony Lambert and Don Bower for their interest and support throughout the program, and Jacques Lebrecque for his invaluable assistance with operations at the Charlevoix Observatory. Benoit Dostaler and Dianne Lemieux maintained the array on a daily basis and John Fahey assisted with data reduction and analysis. H.-J. Kümpel acknowledges the support from a Killam fellowship during a 1-year stay at Dalhousie University, Halifax, Nova Scotia.

References

Agnew, D.C.: Nonlinearity in rock: evidence from earth tides. J. Geophys. Res. **86**, 3969–3978, 1981

Beaumont, C.: Linear and nonlinear interactions between the earth tide and a tectonically stressed earth. In: Applications of geodesy to geodynamics, I. Mueller, ed.: pp 313–318. Ohio State University Press 1978

Brace, W.F., Paulding, B.W., Jr., Scholz, C.H.: Dilatancy in the fracture of crystalline rocks. J. Geophys. Res. **71**, 3939–3953, 1966

Farrell, W.E.: Deformation of the Earth by surface loads. Rev. Geophys. Space Phys. **10**, 761–797, 1972

Flach, D., Große-Brauckmann, W., Herbst, K., Jentzsch, G., Rosenbach, O.: Ergebnisse von Langzeitregistrierungen mit Askania-Bohrlochneigungsmessern – Vergleichende Analyse hinsichtlich der Gezeitenparameter und langperiodischer Anteile sowie instrumentelle Untersuchungen. Deutsche Geodät. Komm. **B211**, (M. Bonatz, ed.) 72–95, 1975

Gallagher, B.S., Munk, W.H.: Tides in shallow water: spectroscopy. Tellus **XXIII**, 346–363, 1971

Godin, G.: Eight years of observations on the water level at Quebec and Grondines 1962–1969. Manuscript Report Series **31**, Marine Sciences Directorate, Dept. Environment, Canada, 1973

Goertzel, G.: An algorithm for the evaluation of finite trigonometric series. Am. Math. Month. **65**, 34, 1958

Harrison, J.C.: Cavity and topographic effects in tilt and strain measurements. J. Geophys. Res. **81**, 319–328, 1976

Mjachkin, V.I., Sobolev, G.A., Dolbilkina, N.A., Morosov, V.N., Preobrazensky, V.B.: The study of variations in geophysical fields near focal zones of Kamchatka. Tectonophysics **14**, 287–293, 1972

Mjachkin, V.I., Brace, W.F., Sobolev, G.A., Dieterich, J.H.: Two models for earthquake forerunners. Pageoph. **113**, 169, 1975

Nersesov, I.L., Semenov, A.N., Simbireva, I.G.: Space-time distribution of the travel time ratios of transverse and longitudinal waves in the Garm area. In: The physical basis of foreshocks, Moscow: Nauka Publ. 1969

Peters, J.A., Beaumont, C.: Borehole tilt measurements from Charlevoix, Quebec. J. Geophys. Res. **90**, 12791–12806, 1985

Rice, J.R., Rudnicki, J.W.: Earthquake precursory effects due to pore fluid stabilization of a weakening fault zone. J. Geophys. Res. **84**, 2177–2193, 1979

Rossiter, J.R., Lennon, G.W.: An intensive analysis of shallow water tides. Geophys. J.R. Astron. Soc. **16**, 275–293, 1968

Scholz, C.H., Kranz, R.: Notes on dilatancy recovery. J. Geophys. Res. **79**, 2132–2135, 1974

Schüller, K.: Tidal analysis by the hybrid least squares frequency domain convolution method. Proceedings of the Eighth International symposium on Earth Tides, M. Bonatz and P. Melchior eds., Institut für Theoretische Geodäsie der Univ. Bonn, FRG, 1977

Sobolev, G., Spetzler, H., Salov, B.: Precursors to failure in rocks while undergoing anelastic deformations. J. Geophys. Res. **83**, 1775–1784, 1978

Soga, N., Mizutani, H., Spetzler, H., Martin III, R.J.: The effect of dilatancy on velocity anisotropy in Westerly granite. J. Geophys. Res. **83**, 4451–4458, 1978

Stuart, W.D.: Diffusionless dilatancy model for earthquake precursors. Geophys. Res. Lett. **1**, 261–264, 1974

Tomaschek, R., Groten, E.: Die Residualbewegung in der horizontalen Gezeitenkomponente. Geofisica Pura e Applicata **56**, 1–15, 1963

Whitcomb, J.H., Garmany, J.D., Anderson, D.L.: Earthquake prediction: variation of seismic velocities before the San Fernando earthquake. Science **180**, 632–635, 1973

Xi, Qinwen: A new complete development of the tide-generating potential for the epoch J2000.0. Bull. Inf. Marées Terrestres **98**, 6744–6747, 1987

Zetler, B.D., Cummings, R.A.: A harmonic method for predicting shallow water tides. J. Marine Res. **25**, 103–114, 1967

Zschau, J.: Auflastgezeiten. Habilitation thesis, Kiel University, 1979

Received June 22, 1987; revised version September 10, 1987
Accepted September 10, 1987